Clinical & Experimental Immunology
The Journal of Translational Immunology

Clinical and Experimental Immunology ORIGINAL ARTICLE doi: 10.1111/cei.13555

FAM96A knock-out promotes alternative macrophage polarization and protects mice against sepsis

A. Yin,*† W. Chen ,*†1 L. Cao,*†1 Q. Li,‡ X. Zhu‡ and L. Wang*†

*Center for Human Disease Genomics, Department of Immunology, Health Science Center, School of Basic Medical Sciences, Peking University, China, †Key Laboratory of Medical Immunology, School of Basic Medical Science, Peking University, Ministry of Health, PR China, and ‡Institute of Chinese Materia Medica, China Academy of Chinese Medical Sciences, Beijing, China

Accepted for publication 13 November 2020
Correspondence: L. Wang, Center for Human Disease Genomics, Department of Immunology, Health Science Center, School of Basic Medical Sciences, Peking University, 38 Xueyuan Road, Beijing 100191, China.
E-mail: wanglu@bjmu.edu.cn
[1]These authors contributed equally to this work and should be considered co-first authors.

Summary

Sepsis is an intractable clinical syndrome characterized by organ dysfunction when the body over-responds to an infection. Sepsis has a high fatality rate and lacks effective treatment. Family with sequence similarity 96 member A (FAM96A) is an evolutionarily conserved protein with high expression in the immune system and is related to cytosolic iron assembly and tumour suppression; however, research has been rarely conducted on its immune functions. Our study found that *Fam96a*$^{-/-}$ mice significantly resisted lesions during sepsis simulated by caecal ligation and puncture (CLP) or endotoxicosis models. After a challenge with lipopolysaccharide (LPS) or infection, *Fam96a*$^{-/-}$ mice exhibited less organ damage, longer survival and better bacterial clearance with decreased levels of proinflammatory cytokines. While screening several subsets of immune cells, FAM96A-expressing macrophages as the key cell type inhibited sepsis development. *In-vivo* macrophage depletion or adoptive transfer experiments abrogated significant differences in the survival of sepsis between *Fam96a*$^{-/-}$ and wild-type mice. Results of the bone marrow-derived macrophage (BMDM) polarization experiment indicated that FAM96A deficiency promotes the transformation of uncommitted monocytes/macrophages (M0) into M2 macrophages, secreting fewer proinflammatory cytokines. FAM96A may mediate an immunometabolism shift – from oxidative phosphorylation (OXPHOS) to glycolysis – in macrophages during sepsis, mirrored by reactive oxygen species (ROS) and glucose uptake. These data demonstrate that FAM96A regulates inflammatory response and provide a novel genomic insight for sepsis treatment.

Keywords: FAM96A, inflammation, macrophage polarization, metabolism, sepsis

Introduction

Sepsis is an intractable and life-threatening condition caused by systemic blood infection, and results in organ damage because of the dysregulation of the immune response [1]. Owing to its high prevalence and mortality worldwide, the World Health Organization (WHO) declared sepsis a global health priority and its overall incidence is still rising [2]. Current therapies are symptomatic treatments, including intravenous fluids administration [3] and organ function support [4], while most aetiological therapies have failed [5]. There is therefore an urgent need for a multi-target therapeutic approach for sepsis.

When infection occurs, pathogenic or conditional pathogenic bacteria invade the bloodstream and produce toxins, enzymes and metabolic products during colonization and growth. The syndrome includes fever, rash, joint swelling, liver and spleen enlargement with migrating lesions in the vast majority, and septic shock in some severe cases. Septic shock characterizes two responses, called systemic inflammatory response syndrome (SIRS) and compensated anti-inflammatory response syndrome (CARS), which are partly caused by the body releasing chemicals into the bloodstream to fight the infection. Key to fighting the infection are the pathogen-associated

molecular patterns (PAMPs) or damage-associated molecular patterns (DAMPS) binding to Toll-like receptor-4 (TLR-4), which facilitates transcriptional activation via myeloid differentiation primary response 88 (MyD88)-dependent and MyD88-independent pathways. This leads to nuclear factor kappa B (NF-κB) and interferon regulatory factor 3 (IRF3) activation and induces the release of chemicals such as nitric oxide (NO) and cytokines. Most of these chemicals are inflammatory cytokines, including proinflammatory tumour necrosis factor-α (TNF-α) and interleukin (IL)-1, IL-6 and IL-12, which can activate the host immune-inflammatory system. However, some are anti-inflammatory cytokines, such as IL-1 receptor antagonist (IL-1ra), IL-4, IL-10 and IL-13, which have the opposite role. A huge release of proinflammatory cytokines can induce vascular endothelial cells to express the adhesion molecules intercellular adhesion molecule 1 (ICAM-1) and vascular cell adhesion protein 1 (VCAM-1), which cause granulocytes and other immune cells to adhere and produce microthrombus. Proinflammatory cytokines can also attract more immunocytes and further cause the production and release of new cytokines, eventually leading to tissue damage and organ dysfunction.

The secretion of cytokines is closely related to immune cells, especially macrophages. Freudenberg *et al.* [6] reported that macrophages can induce tolerance to LPS lethality. After the transformation of uncommitted monocytes/macrophages (M0) into M1 or M2 macrophages, many inflammatory molecules are secreted [7,8]. M1 macrophages are characterized by their enhanced ability to secrete proinflammatory cytokines, such as IL-1β, TNF-α, IL-12 and IL-18, which play a beneficial role in controlling bacterial infections, but also exacerbate inflammatory processes in lethal sepsis [9]. M2 macrophages secrete IL-10, IL-13, C-C motif chemokine ligand (CCL)17 and CCL18, and are usually observed in the later stages of sepsis [10]. IL-10 exerts protective action during systemic inflammation/sepsis owing to its immunosuppressive action [11]. Pena *et al.* [12] revealed the correlation between alternative polarization (M2) and endotoxin tolerance states in human mononuclear cells. Drug intervention based on macrophage immunometabolism could be a therapeutic approach to sepsis [10].

Cytosolic iron–sulphur (Fe/S) assembly component 2A (CIAO2A), also called family with sequence similarity 96 member A (FAM96A), is a homologue of CIA2 containing a domain of unknown function (DUF)59 domain. FAM96A, as both an iron regulatory protein 1 (IRP1)-specific targeting factor and a stabilizing component for IRP2, directly influences cellular iron regulation [13]. Schwamb *et al.* [14] reported that as an apoptosome-activating protein, FAM96A can evoke tumour apoptosis to suppress gastrointestinal stromal tumours. FAM96A also helps to maintain colonic homeostasis and protects against DSS-induced colitis by preventing gut microbial dysbiosis [15].

According to The Human Protein Atlas site, FAM96A has conserved sequences and is widely expressed in many tissues, especially in the immune system. However, research on FAM96A function is still at an early stage. Here, we generated Fam96a knock-out (*Fam96a*$^{-/-}$) mice and aimed to evaluate the role of FAM96A on inflammation. We used two animal models, LPS-induced endotoxaemia and caecal ligation and puncture (CLP), to simulate the clinical process of sepsis. Next, the inflammation cytokine and macrophage polarizations in wild-type (WT) and *Fam96a*$^{-/-}$ mice littermates were analysed. We also performed a gentamicin protection assay and phagocytosis assay in bone marrow-derived macrophages (BMDMs) to enhance the results. Finally, glucose uptake and Western blot analyses were used to reveal the possible mechanism.

Materials and methods

Ethics statement and animals

All animal experiments were approved by the Institutional Animal Care and Use Committee of Peking University and used in accordance with established International Guiding Principles for Animal Research. We crossed *Fam96a*$^{flox/-}$ mice with Zp3-cre mice (both from the Model Animal Research Center of Nanjing University) and generated Zp3-cre-*Fam96a*$^{flox/-}$ female mice, which were then crossed with WT male mice to acquire *Fam96a*$^{+/-}$ mice, from which *Fam96a*$^{-/-}$ and WT mice were bred. All mice in this study were on the C57BL6/J background and used at 8–12 weeks of age. All mice were housed under specific pathogen-free conditions at Peking University Health Science Center.

Antibodies and plasmid

FAM96A anti-serum was raised in rabbits immunized with bacterially expressed, N-terminally GST-tagged and purified full-length proteins. Anti- Ndufs1 (ab169540; abcam, Cambridge, MA, USA), anti-SDHB (ab178423; abcam) and anti-UQCRFS1/RISP (ab191078; abcam) were used in Western blot. pET-RGP plasmid was supplied courtesy of Professor Yingyu Chen, Center for Human Disease Genomics, Peking University.

Validation of the degree of knock-out in the *Fam96a*$^{-/-}$ mice

The mouse *Fam96a* gene has five exons, and the targeting vector was constructed by inserting a Loxp sequence on the two sides of exons 2 and 3 (Supporting information, Fig. S1). The mouse genotyping primers (Table 1) and polymerase chain reaction (PCR) programme (Table 2) are presented as follows.

Table 1. Primers for mouse genotyping

Primers	Sequences
KO-1 (annealing temperature: 64℃)	Forward: GAGTTGCCACATGTTAGTTCCTGTG Reverse: AGACTCAAGCATTTACTCCC
KO-2 (annealing temperature: 64℃)	Forward: AGACCTGCTAAGTCATCCCG Reverse: GAACAAAGGAGCACCACAAA
KO-3 (annealing temperature: 60℃)	Forward: TAGGGCTGTGCCTAAGAGTA Reverse: GTCTTACCGTACTTGACTGC

Table 2. PCR programme for mouse genotyping

95℃	5 min
95℃	30 s
Indicated temperature	30 s
72℃	40 s
72℃	5 min
Repeat 2–4 for 40 cycles	

PCR = polymerase chain reaction.

CLP models

Mice were fasted for 12 h before surgery and anaesthetized with a 2-ml/kg intraperitoneal dose of 2·5% pentobarbital sodium solution. After the abdomens of the mice were shaved and their skin disinfected, a 2-cm midline incision was performed and the caecum was isolated from the mesentery. After the residual faeces of the caecum were carefully milked into the blind end, the caecum was ligated with a septic 4-0 silk braided non-absorbable suture (Mersilk SA83G; Ethicon; Johnson & Johnson Medical Devices Company, New Brunswick, NJ, USA) at the half-length position from the ileocaecal valve to the blind end and perforated twice with a 22-gauge needle distal to the ligation point. Then, the bowel was replaced and the abdominal cavity was closed by running suture. Finally, all the mice were resuscitated by subcutaneous injection with prewarmed normal saline (5 ml/100 g) and returned to their cages.

LPS-challenged endotoxaemia models

A designated dose of sterile lipopolysaccharide saline from *Eschericia coli* (O111:B4; Sigma-Aldrich, St Louis, MO, USA) and the same volume of normal saline were intraperitoneally injected into WT and *Fam96a*$^{-/-}$ mice, respectively.

Bacterial load in the blood and peritoneal cavity

At 6 and 24 h post-CLP operation, blood was sampled from the eyes of the mice and collected in ethylenediamine tetraacetic acid (EDTA) anti-coagulant tubes. For peritoneal lavage, the peritoneal cavity was washed with 3·0 ml of sterile PBS, and the peritoneal lavage fluids were collected. The collected blood and peritoneal fluid were diluted 100-fold and evenly spread on a trypsin blood plate or tryptic soy agar plate (Solarbio, Beijing, China) cultivated in an incubator at 37°C for 24 h. The number of colonies on the plate were then counted.

Induction of BMDMs and polarization

L929 cells were cultured for 3 days in Dulbecco's modified Eagle's medium (DMEM) and supernatants fluids were filtered (0·22 μm) to obtain the L929 medium. WT and *Fam96a*$^{-/-}$ mice bone marrow were isolated from the femur and tibia and cultured in BMDM-conditioned medium [DMEM containing 20% fetal bovine serum (FBS), 20% L929 medium and 100 U/ml penicillin 100 U/ml streptomycin] for 7 days to collect the adherent BMDM cells. For classical (M1) or alternative (M2) macrophage activation, BMDMs were stimulated with murine IFN-γ (100 U/ml) plus LPS (5 ng/mL) or murine IL-4 (10 ng/ml) for 24 h, respectively.

BMDM adoptive transfer and depletion of macrophages

The BMDMs of donor mice were prepared by the use of the aforementioned methods, 2×10^6 of which were resuspended in sterile PBS, then transferred into lethally irradiated (10 Gy) mice intravenously via the lateral tail vein. After 8 h, the two groups were treated with LPS. For the *in-vivo* deletion of macrophages, clodronate liposomes (purchased from Liposoma, Amsterdam, the Netherlands) were shaken evenly just before use, and 0·1 ml of the suspension was intravenously injected per 10 g of mice weight. Mice were challenged with LPS after 48 h.

RNA isolation, reverse transcription and quantitative PCR

Total RNA was isolated and reverse-transcripted using TRIzol™ Reagent and a RevertAid RT reverse transcription kit (Thermo Fisher Scientific, Waltham, MA, USA). Quantitative reverse transcription (qRT)–PCR was performed using FastSYBR mixture (CWBIO, Beijing, China) on a Roche LightCycler 480. All samples were assayed in triplicate. The PCR programme (Table 3) was chosen to compare the cycle threshold (CT) value of the target gene to glyceraldehyde-3-phosphate dehydrogenase (GAPDH) using the formula $2^{-\Delta\Delta CT}$.

Flow cytometry, cytokine and reactive oxygen species (ROS) analysis

For flow cytometry, tissues were processed into single-cell suspensions by a 70-μm cell strainer. Non-specific binding was blocked with anti-CD16/32 (Thermo Fisher Scientific)

Table 3. PCR programme for qPCR

94℃	30 s
94℃	5 s
60℃	30 s
Repeat 2–3 for 40–45 cycles	
Dissociation s	

qPCR = quantitative polymerase chain reaction.

for 10 min on ice. Washed cells were stained for 30 min on ice (CD4 clone RM4-5; CD8a clone 53-6.7; CD19 clone 1D3; CD11b clone M1/70; CD115 clone AFS98; Ly-6G clone 1A8-Ly6g; F4/80 cloneBM8; CD11c clone N418; and CD206 clone MR6F3; all from Thermo Fisher Scientific), then washed twice followed by analysis with a BD FACSVerse™ (BD Biosciences, San Jose, CA, USA) cytometer. Blood samples were left to clot for at least 30 min before centrifugation for 15 min at 4℃ and 1000 ***g***, and supernatant serum were collected. The serum was detected by LEGENDplex™ Mouse Inflammation Panel (BioLegend, San Diego, CA, USA), according to the manufacturer's instructions. For ROS detection, BMDMs were stimulated with LPS (5 ng/ml) for a set time and collected. Then, BMDM were cultured in serum-free medium with a 1 : 1000 dilution of 2′-7′-dichlorofluorescin diacetate (DCFH-DA) (Solarbio) for 37℃ and 30 min, following analysis on the flow cytometer.

Gentamicin protection assay

BMDMs were cultured in BMDM-conditioned medium and seeded in 60-mm tissue culture plates (REF#430166; Corning, New York, NY, USA). pUC19 plasmid was transformed into *E. coli* BL21, cultured overnight in Luria–Bertani liquid medium with 100 μg/ml ampicillin (LA). BMDMs were overlaid with the inoculum at a multiplicity of infection (MOI) of 10 and incubated for 30 min. Two identical plates for time-points 0 h (T0) and 3 h (T3) were set up during each experiment. The supernatants were aspirated and cells were washed three times with PBS. Then, 3 ml of BMDM-conditioned medium with gentamicin (200 μg/ml) (Solarbio) was added. The T0 and T3 plates were incubated at 37°C in a 5% CO_2 atmosphere for 15 min and 3 h, respectively, after which the supernatants were removed entirely by aspiration and washed three times with PBS. Cells were lysed with 2 m of 0·22 μm filter sterilized 1% saponin in distilled water by incubating for 10 min at room temperature (20~30°C), followed by vigorous pipetting. Then, 30 μl of lysates were smeared to solid LA plates to determine the number of intracellular bacteria {% killing = [(T0 – T3)/T0] × 100}. This protocol is adapted from Subashchandrabose *et al.* [16]. We used pUC19 plasmid and LA plates to avoid microbial contamination. Generally speaking, short infection times after the gentamicin treatment (typically 1 h) reflect the bacterial capacity to enter host cells only, while longer infection times after gentamicin treatment (2 h or more) reflect the bacterial capacity to survive and multiply within the target cell as well as the capacity to invade [17]. Image J (Fiji; https://imagej.net/Fiji) was used to perform digital enhancement (plugin: Trainable Weka Segmentation).

Phagocytosis assay and NBDG uptake experiment

pET-RGP plasmid was transformed into *E. coli* BL21 with 0·5 mM isopropyl β- d-1-thiogalactopyranoside (IPTG) induction overnight at 28°C. BMDMs were overlaid with the inoculum at an MOI of 50 and incubated for 3 or 5 h and an MOI of 10 for 5 h. Phagocytosis was detected using a flow cytometer.

For the NBDG uptake experiment, the cells were incubated in BMDM-conditioned medium (without glucose) with 50 μM 2-NBDG (Thermo Fisher Scientific) for 15 min.

Histological analysis

The lungs were fixed in 4% paraformaldehyde for at least 24 h and then embedded in paraffin. Then, 3·5-μm thick tissue sections were sliced for haematoxylin and eosin (H&E) staining, according to standard procedures.

Statistical analysis

All experiments were repeated in triplicate. Normality test and unpaired two-tailed Student's *t*-test of statistics were calculated by GraphPad Prism version 8 (GraphPad Software, San Diego, CA, USA). $P < 0{\cdot}05$ was considered to show a statistically significant difference ($^{*}P < 0{\cdot}05$; $^{**}P < 0{\cdot}01$; $^{***}P < 0{\cdot}001$).

Results

FAM96A knock-out protects against organ damage from sepsis and significantly prolongs survival

To study the role of FAM96A during endotoxin challenge *in vivo*, *Fam96a*$^{-/-}$ and WT mice were challenged with an intraperitoneal injection of LPS to mimic endotoxaemia in humans. The degree of knock-out in the *Fam96a*$^{-/-}$ mice was validated using PCR and Western blot analyses (Supporting information, Fig S2).

We found that the *Fam96a*$^{-/-}$ mice can resist LPS completely, and all survived (Fig. 1a). H&E staining was performed to histologically characterize lung injuries in *Fam96a*$^{-/-}$ and littermate WT mice. *Fam96a* knock-out considerably protected the mice from lung injuries, demonstrating the thickening of the alveolar septa and

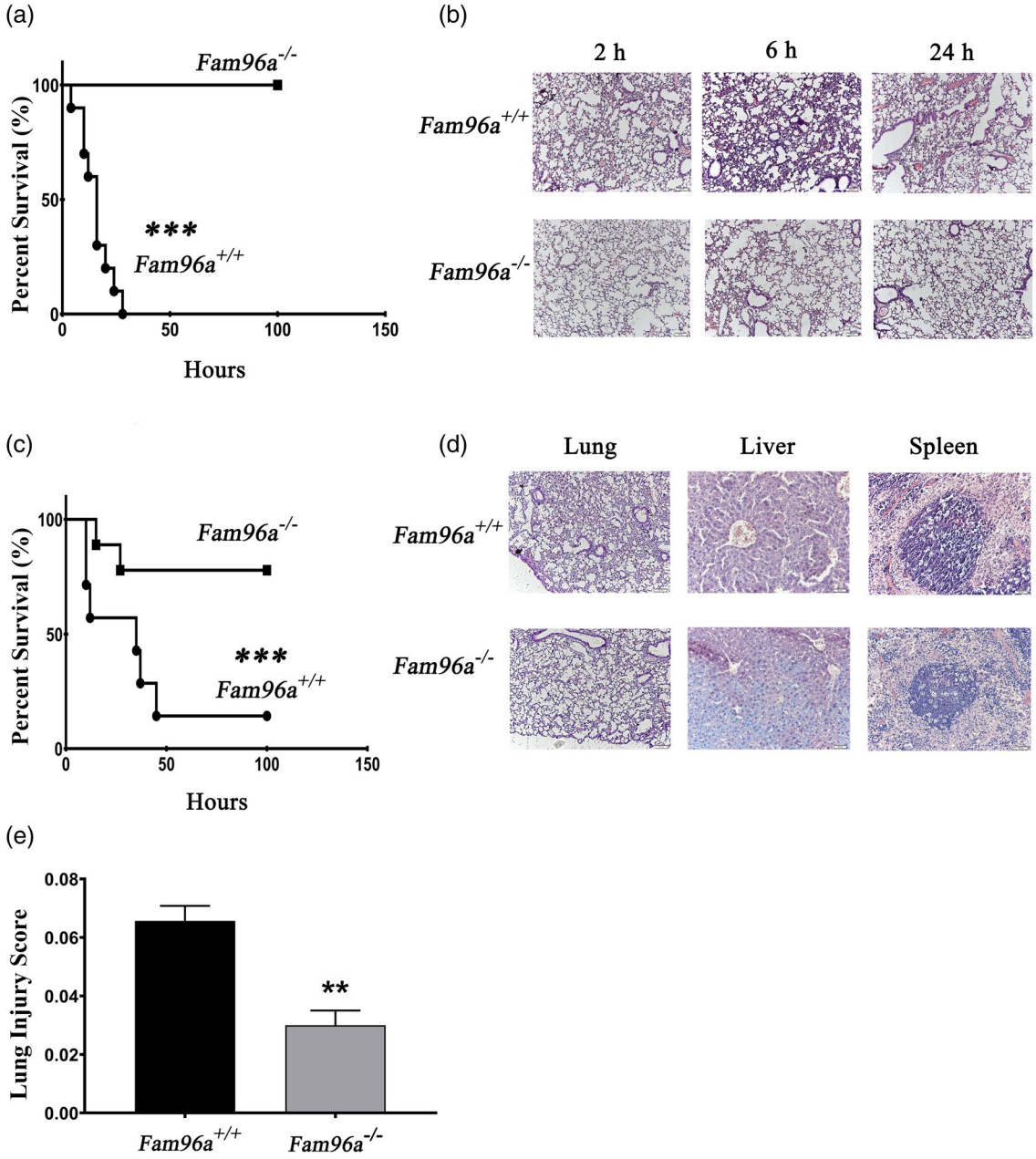

Fig. 1. *Fam96a*$^{-/-}$ mice resist lipopolysaccharide (LPS)-induced endotoxaemia and caecal ligation and puncture (CLP)-induced sepsis. (a) Wild-type (WT) and *Fam96a*$^{-/-}$ mice ($n = 20$) were injected intraperitoneally (i.p.) with LPS (30 mg/kg) and the survival rate was evaluated using the log-rank test. (b) Haematoxylin and eosin (H&E) staining was performed on the lung tissues at 2, 6 and 24 h after WT and *Fam96a*$^{-/-}$ mice ($n = 20$) were injected i.p. with LPS (8 mg/kg). (c) The survival rate of WT and *Fam96a*$^{-/-}$ mice ($n = 9$) was evaluated using the log-rank test after CLP surgery. (d) H&E staining was performed on the lung, liver and spleen 24 h after CLP surgery. (e) Quantitative analysis of the lung tissue injury from CLP-treated WT and *Fam96a*$^{-/-}$ mice at 24 h was performed using the lung injury scoring system, assessing five different parameters: neutrophils in alveolar airspace, neutrophils in the interstitial space, hyaline membranes, proteinaceous debris filling the airspace and alveolar septal thickening. Data are expressed as an independent experiment. $^{*}P < 0{\cdot}05$, $^{**}P < 0{\cdot}01$, $^{***}P < 0{\cdot}001$.

neutrophil infiltration (Fig. 1b). LPS-induced endotoxaemia does not reflect all aspects of sepsis, and the CLP model is considered the gold standard for sepsis research because of the adjusted severity and identified stages [18,19]. We therefore utilized CLP models to study the role of FAM96A during sepsis and quantified the histological changes in

tissue injury using the lung injury scoring system as described [20]. The results were consistent; *Fam96a*$^{-/-}$ mice showed little lung, liver, and spleen damage with lower lung injury scores.

FAM96A knock-out reduces proinflammatory cytokines and bacterial load during sepsis

Given these observations in mice, we tested the serum inflammatory cytokines in *Fam96a*$^{-/-}$ and WT mice in both models. Upon LPS stimulation, rapid rises in proinflammatory cytokine [IL-6, IL-12, IFN-γ and monocyte chemoattractant protein-1 (MCP-1)] responses were observed in WT mice, which peaked at 2 h and subsequently decreased. Although these serum proinflammatory cytokines in *Fam96a*$^{-/-}$ mice also increased in 2 h, they increased far slower than those in WT mice, whereas the anti-inflammatory IL-10 remained at comparable levels in both groups (Fig. 2a).

Decreased levels of TNF-α, IFN-γ, IL-6 and MCP-1 expression were observed in the serum of *Fam96a*$^{-/-}$ mice compared to their littermate controls after CLP surgery (Fig. 2b). The IL-12 levels were inconsistent in the endotoxaemia and CLP experiments, and this may be partly accounted for by the differences in the models.

To analyse the pathological changes in the internal organs in *Fam96a*$^{-/-}$ mice and WT mice during sepsis development, their inflammation cytokines mRNA levels were detected by qRT–PCR. Fam96a induced a high IL-6 mRNA expression in the lung 6 h post-LPS injection (Fig. 2c).

In addition, a diminished bacterial load in the whole blood and peritoneal cavity was observed in *Fam96a*$^{-/-}$ mice, suggesting that Fam96a knock-out enhances the purge of bacteria (Fig. 2d).

FAM96A affects the progression of sepsis through macrophages

To further investigate the relevant cell compartment responsible for resistance to sepsis in *Fam96a*$^{-/-}$ mice, we used flow cytometry to analyse the subtypes of immunocytes 24 h after CLP surgery. The amounts of CD4 T cells, CD8 T cells, CD19 B cells, neutrophils and monocyte/macrophages were similar between the two groups (Fig. 3a,b). This result was also consistent with the immunocyte phenotypes in LPS-induced endotoxaemia (Fig. 3c).

Macrophages play an important role in immune homeostasis and the inflammatory process [10], and macrophages are the major cells that produce various cytokines [21], so we hypothesized that FAM96A controls the immunometabolism of macrophages. BMDMs from *Fam96a*$^{-/-}$ and WT mice were stimulated with LPS and culture supernatants were analysed (the differentiation efficiency of BMDMs has been confirmed by CD11b and F4/80 using flow cytometry) (Supporting information, Fig. S3).

As expected, lower IL-6, MCP-1 and TNF-α levels were produced by BMDMs from *Fam96a*$^{-/-}$ mice after LPS challenge for 24 h, and macrophages from WT mice produced less IL-10 (Fig. 4a). To further evaluate this hypothesis, we designed the adoptive transfer experiment and transferred *Fam96a*$^{-/-}$ and WT BMDMs into *Fam96a*$^{-/-}$ mice. After 8 h of recovery, these mice were challenged with LPS. We found that *Fam96a*$^{-/-}$ mice transplanted with WT BMDMs all died within 25 h while the *Fam96a*$^{-/-}$ BMDM group mice survived (Fig. 4b). We also used clodronate to delete endogenous macrophages following the LPS challenge, and the survival rate of *Fam96a*$^{-/-}$ mice significantly decreased (Fig. 4c).

The data suggest that the loss of FAM96A plays a protective role against sepsis through macrophages, resulting in a decreased mortality, bacterial load and proinflammatory cytokine production.

FAM96A regulates the transformation of uncommitted macrophages (M0) into M1 macrophages

Macrophages can mediate endotoxin tolerance because of the shift towards the M2 macrophage or alternatively activated macrophage (AAM) phenotypes, which contributes to the immunosuppression observed during the later stages of sepsis [10,22–24]. BMDMs from *Fam96a*$^{-/-}$ and WT mice were stimulated with IL-4 to promote M2 macrophages, and with IFN-γ and LPS for M1 macrophages. We then used inducible nitric oxide synthase (iNOS) (NOS2) and arginase 1 (Arg-1) as evaluation criteria to assess the degree of polarization of M1 and M2, respectively. The results revealed that the BMDMs from *Fam96a*$^{-/-}$ mice preferred M2 differentiation to M1 polarization (Fig. 5a), while the opposite was true for the BMDMs from WT mice (Fig. 5c). Next, we performed flow cytometric analyses using typical M1 and M2 markers (CD206 and CD11c) gated in conventional macrophages (F4/80^{+}, CD11b^{+}) to investigate the BMDM polarization. We observed a decreased number of M1 macrophages (CD11c^{+}, CD206^{-}) in BMDMs from *Fam96a*$^{-/-}$ mice after LPS and IFN-γ stimulation, while M2 macrophages increased after IL-4 stimulation (Fig. 5b,d). These results indicate that FAM96A may play a crucial part in the shift of macrophages towards M2 phenotype differentiation.

FAM96A modulates ROS metabolism of macrophages

Finally, we evaluated the ROS in the BMDMs of *Fam96a*$^{-/-}$ and WT mice. The shift in cellular metabolism from

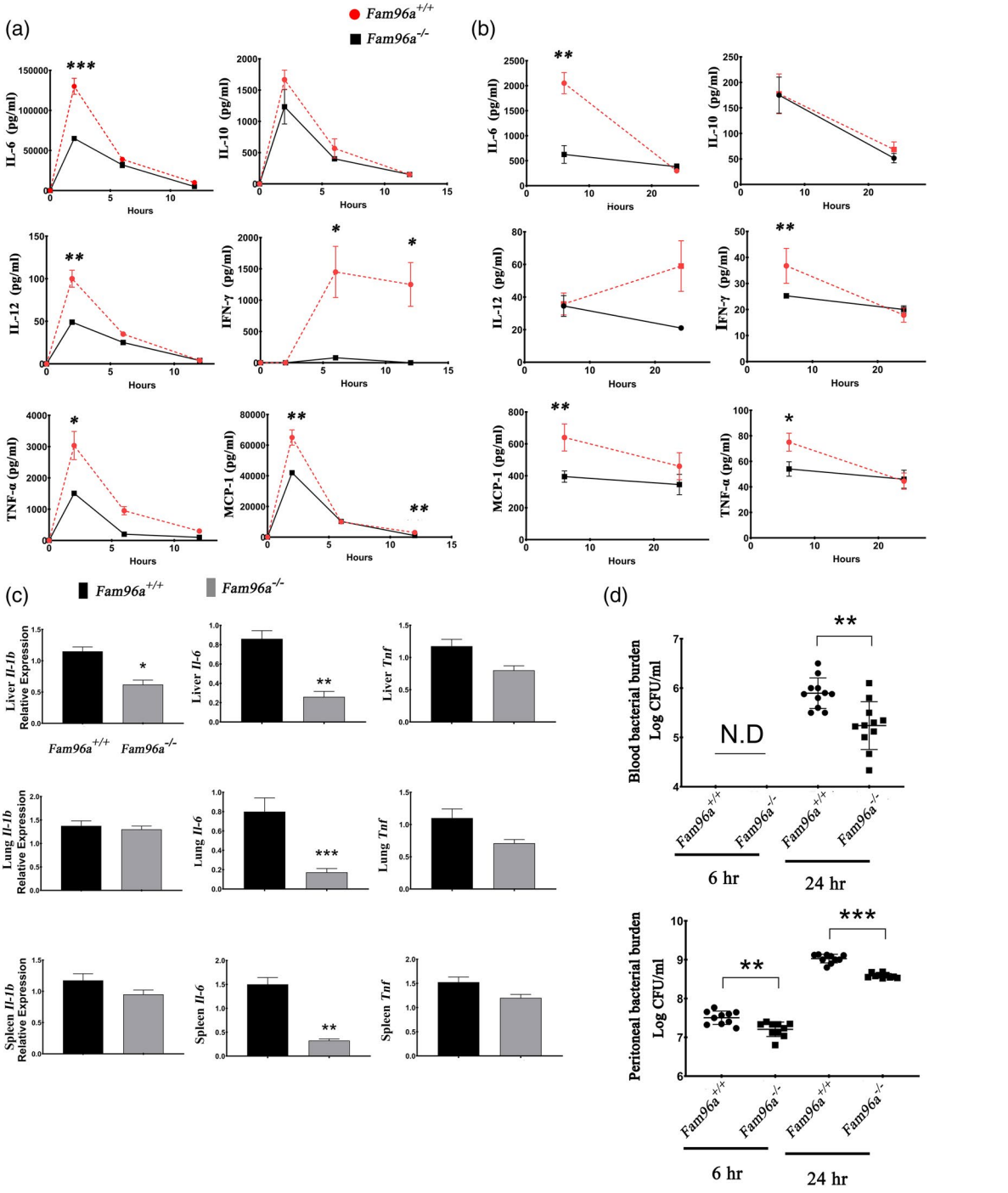

Fig. 2. Family with sequence similarity 96 member A (FAM96A) deficiency reduced proinflammatory cytokines and bacterial load during sepsis. (a) Wild-type (WT) and *Fam96a*$^{-/-}$ mice (n = 20) were injected intraperitoneally (i.p.) with lipopolysaccharide (LPS) (15 mg/kg) and serum cytokine concentrations were analysed at 2, 6 and 12 h. (b) WT and *Fam96a*$^{-/-}$ mice (n = 10) were exposed to caecal ligation and puncture (CLP) surgery and serum cytokine concentrations were analysed at 6 and 24 h. (c) WT and *Fam96a*$^{-/-}$ mice (n = 20) were injected i.p. with LPS (15 mg/kg) and interleukin (IL)-1b, tumour necrosis factor (TNF) and IL-6 mRNA expression levels in the lung, spleen and liver were determined by quantitative reverse transcription–polymerase chain reaction (qRT–PCR) and standardized to those of glyceraldehyde 3-phosphate dehydrogenase (GAPDH) after 2–2·5 h. (d) The bacterial burden in the blood and peritoneal lavage fluid were measured at the indicated time-points after CLP surgery. Data are expressed as the means ± standard error of the mean (s.e.m.) of an independent experiment. *P < 0·05, **P < 0·01, ***P < 0·001; n.d. not detected.

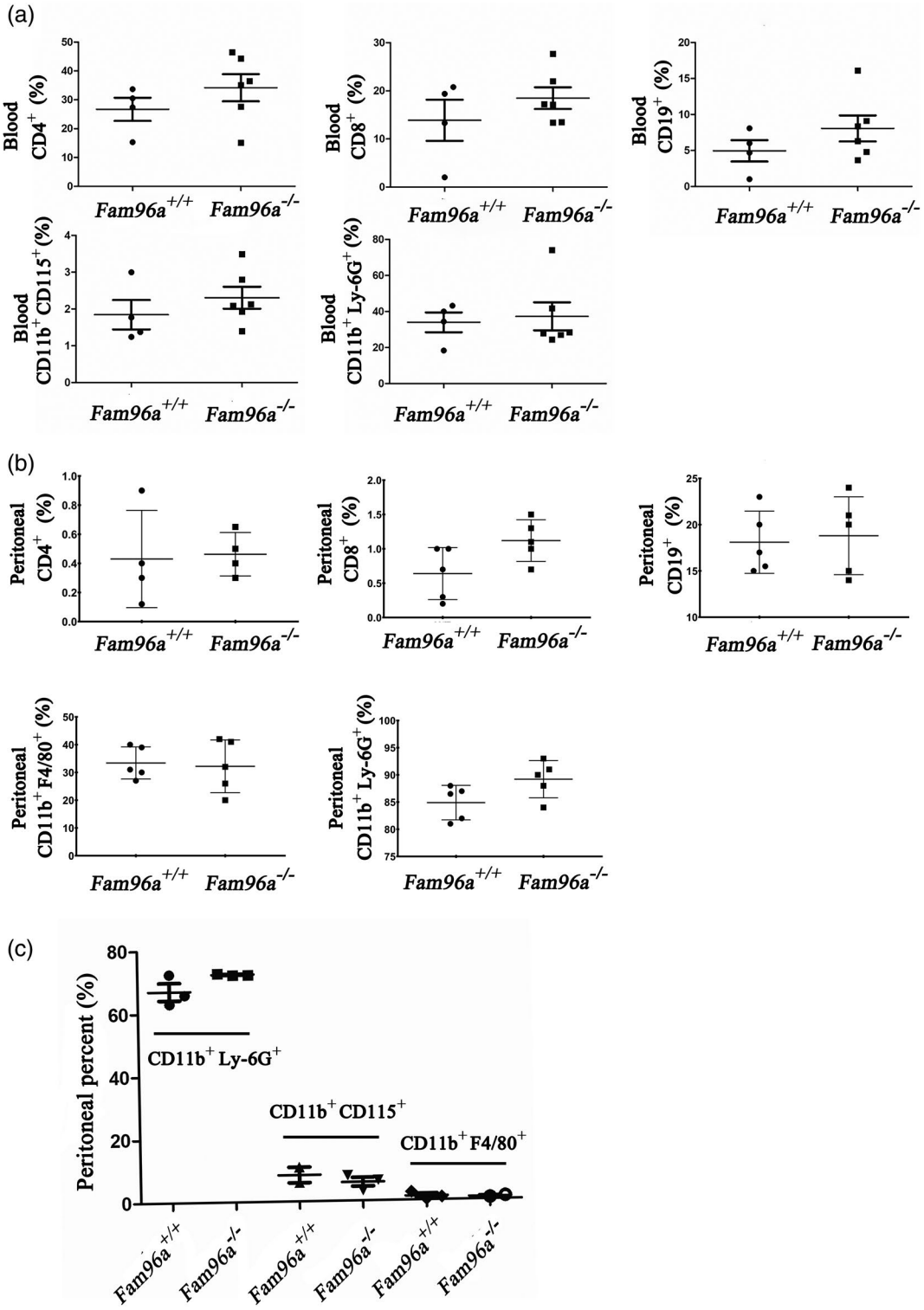

Fig. 3. *Fam96a*$^{-/-}$ mice showed no significant changes in blood and peritoneal immune cell subsets. The indicated immunocytes of blood (a) and peritoneal cavity (b) were analysed by flow cytometry in *Fam96a*$^{-/-}$ and wild-type (WT) mice 24 h after caecal ligation and puncture (CLP) surgery. (c) The indicated immunocytes of the peritoneal cavity were analysed by flow cytometry in *Fam96a*$^{-/-}$ and WT mice 24 h after lipopolysaccharide (LPS) challenge [intraperitoneal (i.p.) injection, 15 mg/kg]. Data are expressed as the means ± standard error of the mean (s.e.m.) of an independent experiment.

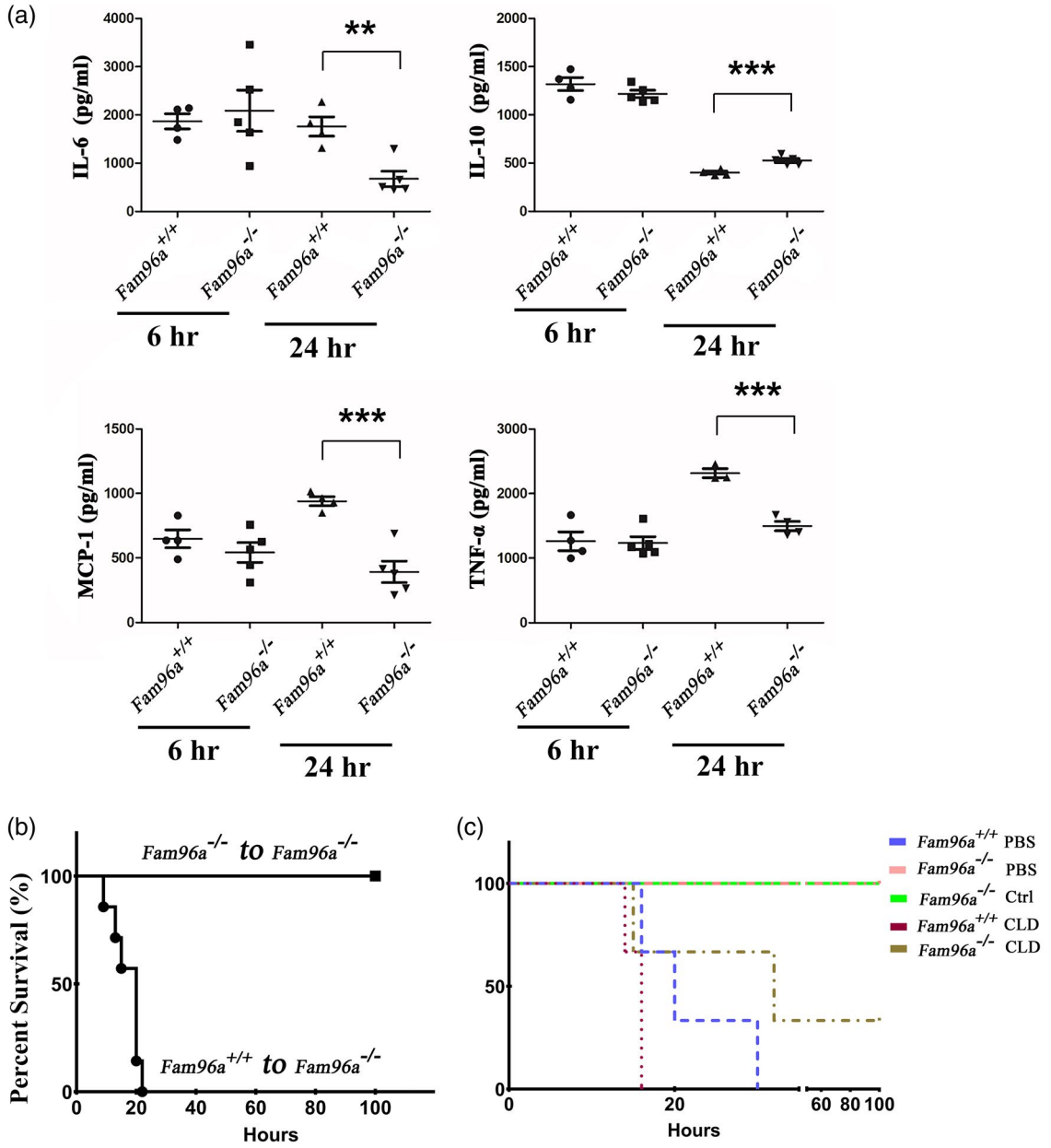

Fig. 4. Family with sequence similarity 96 member A (FAM96A)-deficient macrophages ameliorate inflammation state and improve survival during sepsis. (a) Bone marrow-derived macrophages (BMDMs) were stimulated with lipopolysaccharide (LPS) (100 ng/ml) for 6 and 24 h and concentrations of tumour necrosis factor (TNF)-α, monocyte chemoattractant protein-1 (MCP-1), interleukin (IL)-10 and IL-6 in the supernatant were measured. (b) BMDMs from wild-type (WT) or *Fam96a*$^{-/-}$ mice were intravenously transferred into the recipient *Fam96a*$^{-/-}$ mice (n = 10). After 8 h, the two groups were treated with LPS (15 mg/kg) and the survival rate was assessed using the log-rank test. (c) Macrophages of WT and *Fam96a*$^{-/-}$ mice were exhausted by clodronate and phosphate-buffered saline (PBS) was used to control the variables. Control means that neither clodronate nor PBS was injected in mice. The survival rate was assessed using the log-rank test after LPS challenge (15 mg/kg). Data are expressed as the means ± standard error of the mean (s.e.m.) of an independent experiment. *P < 0·05, **P < 0·01, ***P < 0·001.

oxidative phosphorylation (OXPHOS) to glycolysis (the Warburg effect) is required to transform M0 macrophages to M1 because of the urgent need for ATP production, which is responsible for clearing pathogens and generating inflammatory cytokines. The increased synthesis of ROS can partly reflect this shift, as succinic acid accumulation in mitochondria leads to further oxidation owing to the action of succinate dehydrogenase (SDH) [10,25]. As expected, BMDM stimulation with LPS resulted in lower ROS activity in *Fam96a*$^{-/-}$ mice compared to that in WT

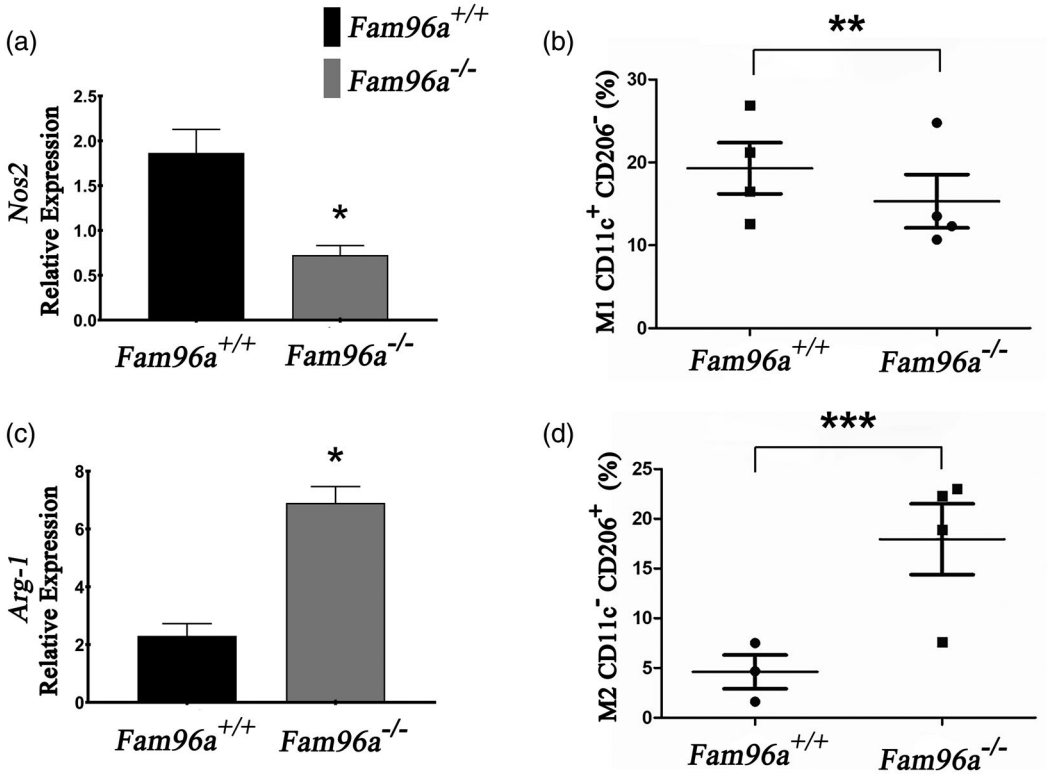

Fig. 5. Family with sequence similarity 96 member A (FAM96A) mediates macrophage polarization and contributes to M1 differentiation after challenge. Bone marrow-derived macrophages (BMDMs) were stimulated with interferon (IFN)-γ (100 U/ml) plus lipopolysaccharide (LPS) (5 ng/ml) for 24 h. M1 macrophage-related gene *Nos2* mRNA expression was determined (a) and characteristic markers ($CD11c^+$ and $CD206^-$) used to define M1 macrophages were analysed by flow cytometry (b). BMDMs were stimulated with interleukin (IL)-4 (10 ng/ml) for 24 h. The M2 macrophage-related gene *Arg-1* mRNA expression was determined (c) and characteristic markers ($CD11c^-$ and $CD206^+$) used to define M2 macrophages were analysed by flow cytometry (d). Data are expressed as the means ± standard error of the mean (s.e.m.) of an independent experiment. $^*P < 0{\cdot}05$, $^{**}P < 0{\cdot}01$, $^{***}P < 0{\cdot}001$.

mice (Fig. 6a). This result showed that FAM96A may control macrophage polarization through OXPHOS to glycolysis transformation. ROS are highly anti-microbial against Gram-positive and Gram-negative bacteria, viruses and fungi and contribute both directly and indirectly to the killing of microorganisms in host defence. To confirm our results, we performed the gentamicin protection assay to determine bacterial survival within BMDMs (Fig. 6b). The plate counts reflected the number of bacteria that entered and survived within BMDMs for 30 min (T0) or 3 h (T3), respectively. As expected, the intracellular bacterial survival numbers increased at 3 h and the ratio of killing percentages within BMDMs from *Fam96a*$^{-/-}$ mice decreased (Fig. 6c), suggesting ROS production and defective intracellular anti-bacterial function. We also used the phagocytosis assay to measure the uptake of bacteria by BMDMs, and the knock-out of *Fam96a* did not appear to cause any difference (Fig. 6d).

Cellular respiration and metabolic processes are the two major sources of ROS production, in which oxygen is reduced by the successive transfer of single electrons, and the intermediates with odd electrons can escape the chain [26]. Since Stehling *et al.* [13] reported that FAM96A may mediate the maturation of cytosolic and nuclear Fe/S proteins as cytosolic Fe/S protein assembly (CIA) apparatus, given the fact that three of the four respiratory chain complexes (complexes I, II and III) are Fe/S proteins with Fe/S cluster co-factors, we detected that the Fe/S cluster contained subunits of complexes I, II and III in the bone marrow of naive *Fam96a*$^{-/-}$ and WT mice. What interested us is that NDUFS1 (complex I) and SDHB (complex II) showed no conspicuous differences, but the expression of UQCRFS1/RISP (complex III) decreased significantly in *Fam96a*$^{-/-}$ mice. UQCRFS1/RISP is the Fe/S cluster subunit [*Uqcrfs1* encodes Rieske iron–protein (RISP)], which is required for the transfer of electrons downstream of complex III as well as complex III ROS production [27]. This suggests that FAM96A mediates macrophage polarization and ROS production through cellular respiration and metabolic processes.

Finally, we explored the glucose uptake of LPS-stimulated BMDMs by 2-NBDG, a fluorescent glucose analogue used

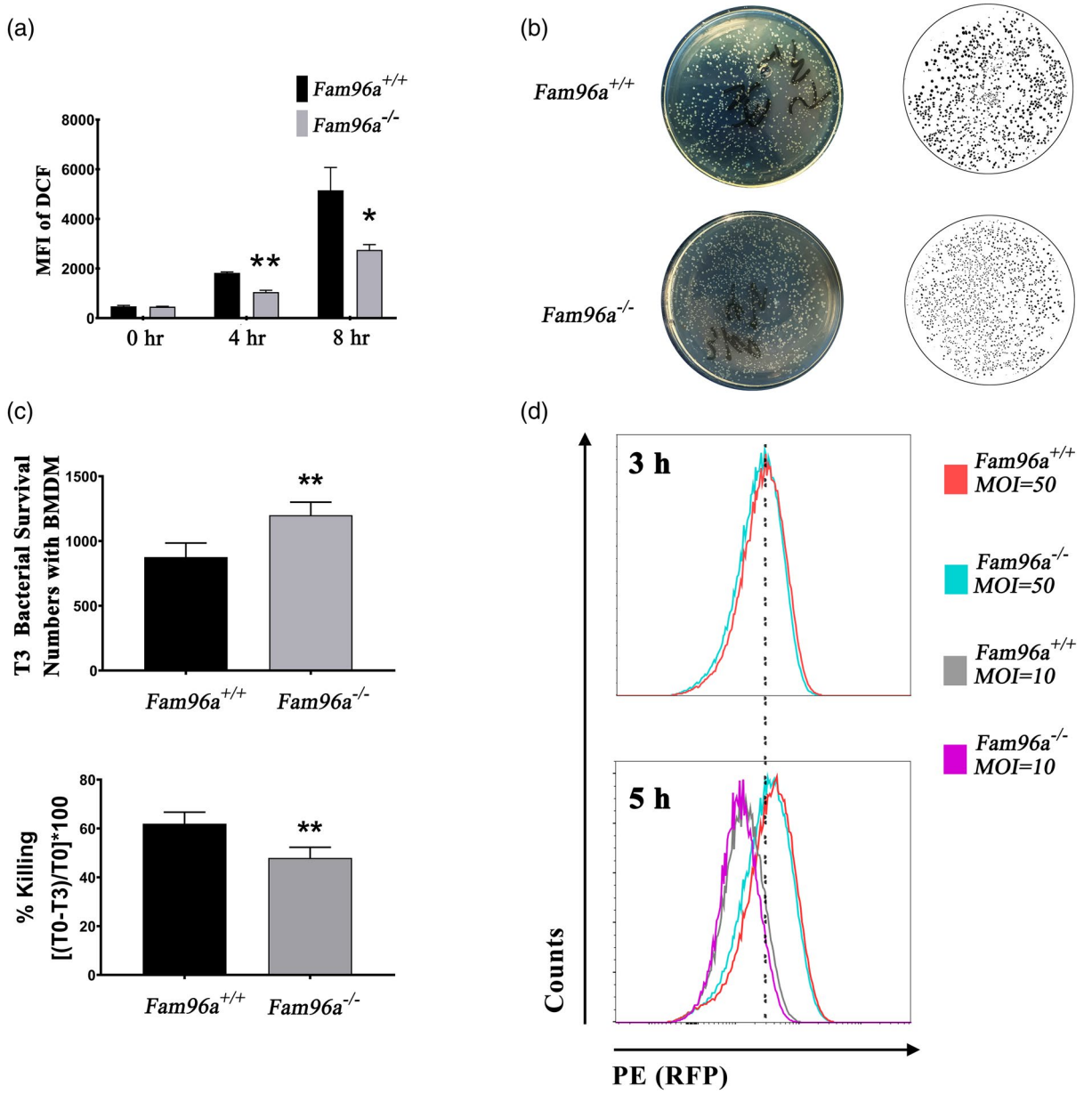

Fig. 6. Family with sequence similarity 96 member A (FAM96A)-deficient macrophages have low reactive oxygen species (ROS) activity and bactericidal function. (a) The ROS activity of bone marrow-derived macrophages (BMDMs) was measured by 2′-7′-dichlorofluorescin diacetate (DCFH-DA) at the indicated time-points after lipopolysaccharide (LPS) treatment (100 ng/ml). Data are expressed as the means ± standard error of the mean (s.e.m.) of an independent experiment. $^{*}P < 0{\cdot}05$, $^{**}P < 0{\cdot}01$, $^{***}P < 0{\cdot}001$. (b) The bacterial survival within BMDMs was determined by gentamicin protection at 3 h. Image J was used to process and enhanced the pictures. (c) Bacteria survival numbers within BMDMs at 3 h and percentage killing of intracellular bacteria were measured. (d) Phagocytosis assay to measure the uptake of bacteria by BMDMs at multiplicity of infection (MOI) 10 and MOI 50.

to monitor glucose uptake in live cells. We measured the glucose uptake at three time-points, 2, 4 and 8 h, after the addition of 100 (Fig. 7b,c) or 250 ng/ml (data not shown) of LPS, and found that it reached its maximum at 4 h, then gradually decreased to the baseline at 8 h in both types of mice. It is obvious that the glucose uptake in *Fam96a*$^{-/-}$ mice was decreased at 4 h, but only slightly decreased at 2 h and seemed to show no change at 8 h.

Discussion

The results of this study reveal a correlation between FAM96A and the development of sepsis. Here, we generated *Fam96a*$^{-/-}$ mice to investigate the function of FAM96A in inflammation using two sepsis models. *Fam96a*$^{-/-}$ mice had significant resistance to organ lesions of sepsis, including haemorrhages, leucocyte infiltration and alveolar

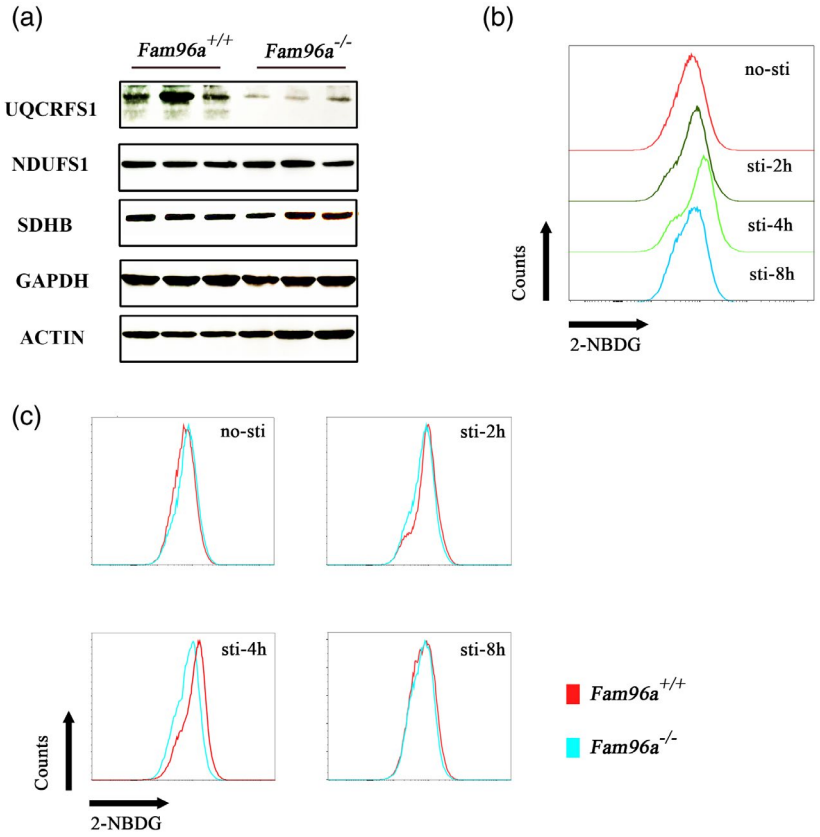

Fig. 7. Family with sequence similarity 96 member A (FAM96A) deficiency impairs iron–sulphur (Fe/S) cluster subunit of respiratory chain complex III and influences the glucose uptake. (a) The bone marrow of naive mice was subjected to immunostaining for the Fe/S clusters containing subunits of complexes I, II and III. (b) The profile of glucose uptake in basal and lipopolysaccharide (LPS)-treated bone marrow-derived macrophages (BMDMs) at 2, 4 and 8 h were measured. (c) Glucose uptake in LPS-treated BMDMs of *Fam96a*$^{-/-}$ and WT mice at several time-points.

capillary membrane thickening, compared to WT mice. All *Fam96a*$^{-/-}$ mice survived after challenge with indicated doses of LPS in our experiments, and deaths of CLP models dropped by more than three times. These results indicate that FAM96A is essential for sepsis outcomes, and its depletion helps to improve survival. Previous studies have suggested that there are moderate genetic influences on the risk of dying by infections, and only a small (if any) effect of the family environment [28]. One study on the relation of infection mortality between adoptees and biological parents as well as that between adoptees and adoptive parents [29] reported that the incidence of sepsis has a significant genetic background. The importance of genetic components in sepsis has been previously reported.

The secretion of inflammatory cytokines was investigated both in endotoxaemia and CLP models. Our results show that Fam96a knock-out reduced the levels of IL-6, MCP-1, IFN-γ and TNF-α. It has been reported that the administration of endotoxin can elevate TNF-α levels in both human and animal subjects [30], and exogenous TNF-α results in a shock state. As one of the current therapeutic agents, targeting TNF-α in those with a high risk of mortality is highly beneficial [31]. Decreased production of TNF-α in *Fam96a*$^{-/-}$ mice may correlate with lower levels of inflammation. The IL-6 level reflects sepsis severity [32]. IL-6 and IL-12 activate the immune-inflammatory system and elevate the progression of sepsis [33], so less of both may lead to a lower host reaction to infections and prolong the survival period. MCP-1, as a proinflammation mediator, was also reduced in *Fam96a*$^{-/-}$ mice. Ramnath *et al.* [34] reported that a blocker of MCP-1 synthesis, bindarit, significantly protects mice against sepsis and endotoxaemia, which means that lower MCP-1 levels are associated with better outcomes. The cytokine difference between *Fam96a*$^{-/-}$ and WT mice disappeared 24 h after LPS challenge or CLP surgery. The main inflammatory factors (TNF-α, IL-6, IL-1β, etc.) in clinical patients also have similar characteristics, rapidly peaking at between 1·5 and 2 h after the onset of sepsis, quickly dropping to their base levels (almost undetectable) after 6 h [35]. Increased levels of the pro-inflammation cytokine IL-12 in *Fam96a*$^{-/-}$ mice were only

found in the endotoxaemia experiment, whereas the anti-inflammatory IL-10 remained at comparable levels in both models. IL-12 levels were inconsistent in endotoxaemia and CLP experiments which might, in part, be attributed to the different mechanisms for simulating sepsis.

Although FAM96A can regulate the production of cytokines during sepsis, we speculated that FAM96A may control the function of a certain cell type to affect the secretion of cytokines. Macrophages play a crucial role in the host defence against a variety of pathogens and the inflammatory immune response during sepsis [36]. We therefore stimulated BMDMs from *Fam96a*$^{-/-}$ and WT mice with LPS and analysed the cultured supernatants. In accordance with previous results, the BMDMs from *Fam96a*$^{-/-}$ mice presented a decrease in proinflammatory cytokines. The transferred BMDMs from WT mice reversed the endotoxin tolerance of *Fam96a*$^{-/-}$ mice, together with the result of the macrophage depletion experiment, demonstrating that *Fam96a* knock-out in macrophages had a protective effect against inflammation. Macrophages polarize to different phenotypes in different metabolic pathways. Classically activated (M1) macrophages secrete proinflammatory cytokines and ROS/reactive nitrogen species (RNS) to activate the immune response and clear pathogens. Alternatively activated (M2) macrophages are ubiquitous in the immunoparalysis stages of sepsis [22], which mediates immunosuppression status [12]. Based on the BMDM polarization experiment, we found that macrophages lacking FAM96a have a robust potential for M2 polarization under challenging conditions and the simultaneous expression of M2 macrophage markers.

Conclusion

Under normal conditions, macrophages use OXPHOS as the main metabolic pathway to maintain their energy requirements. Once stimulated by LPS, lipoteichoic acid and peptidoglycan (PGN), or after contact with some cytokines, macrophages shift from OXPHOS to glycolysis for the rapid synthesis of ATP to meet the higher energy requirements against pathogens (the Warburg effect) [37]. The polarization of M1 and M2 is closely related to the Warburg effect. The polarization of M1 is more dependent upon glycolysis and glutamine decomposition [38,39], while the metabolic reprogramming of M2 is more inclined towards fatty acid oxidation [40,41] and OXPHOS [42]. As FAM96A has been reported to be related to the assembly of Fe/S protein in cells, which is essential in the oxidative respiratory chain [13], FAM96A is likely to affect the oxidative phosphorylation process and cause different directions of macrophage polarization. An increase in glutamine uptake and its metabolism is also reported in M1 macrophages [10,39,43]. A higher uptake of glutamine generates more α-ketoglutarate, which is used by the tricarboxylic acid cycle (TCA) cycle for increased succinate production. Furthermore, the accumulation of succinic acid in mitochondria leads to further oxidation owing to the action of SDH, causing an increased synthesis of ROS. It has been reported that the increased generation of intracellular NO by macrophages for more than 12 h damages their mitochondrial electron transport chain [44]; thus, the activity of ROS can partly reflect the Warburg effect [10]. We found that the loss of FAM96A in BMDMs dampened the ROS activity. Here, we hypothesize that FAM96A controls macrophage polarization through glycolysis–OXPHOS transformation and ROS.

Reprogramming of intracellular metabolisms is required for the proper polarization and function of activated macrophages [45]. The metabolic process of tumour cells is similar to that of activating immune cells, except that the latter can transition between resting catabolic states (for example, naive and memory T cells) to one of growth and proliferation (for example, effector T cells) as part of a normal developmental programme [46]. Glycolysis, the TCA cycle and electron transport chain, as three main processes, control the efficiency and method of energy production. As CIA apparatus, we found that FAM96A may control the expression of complex III, even in the naive status (naive mice), and influence the uptake of glucose under stress conditions (LPS treatment). It is known that complexes I, II and III of the mitochondrial electron transport chain can generate ROS [47], partly because of 'leakage'. ROS can also mediate the signalling intermediates controlling T cell activation [27], but little is known about whether ROS reduction in M2 macrophages is the cause or the result of polarization. Analysis of the oxygen consumption rate and extracellular acidification rate (ECAR), including the enzyme activity of complex III, could provide more direct evidence; however, because of restrictive experimental conditions, this study has not yet been performed. This will be investigated further in our future studies.

It is certain that targeting the degree of sepsis progress and the time-point of M1/M2 transformation is crucial to the outcome. Zhang *et al.* [48] reported that targeting enzymes involved in the glycolytic pathway in M1 macrophages may prove beneficial, depending on the immunological stage.

To the best of our knowledge, our study is the first to investigate the role of FAM96A in sepsis. Knock-out of the *Fam96a* gene in mice resulted in an effective prolonged survival, leading to minor damage in the lungs, which can be explained by the changes in sepsis-associated cytokines. *Fam96a*$^{-/-}$ macrophages have the potential for M2 differentiation, which can alleviate the levels of proinflammatory cytokines in the early sepsis stage. FAM96A may affect the OXPHOS pathway shifting during macrophage transformation. Previous studies have revealed the

conserved expression and functions of FAM96A in tissues and tumours, while few underlying mechanisms have been elucidated in the immune system. Our study provides novel genetic insights into the mechanism of sepsis and a potential therapeutic target for clinicians.

Acknowledgements

This work was supported by grants from the National Natural Science Foundation of China (No. 91542106).

Disclosures

The authors have no conflicts of interest to declare.

Author contributions

A. Y. designed the studies and performed experiments and data analysis. W. C. designed the studies and conducted experiments, including data analysis, especially for mechanisms. W. C. wrote the manuscript. A. Y. and W. C. contributed equally to this work and should be considered co-first authors. L. C. assisted with some animal experiments. Q. L. and X. Z. revised the manuscript and contributed to some experimental reagents and equipment use. L. W. contributed to essential discussions, provided ideas, revised the manuscript and supervised the work.

Data Availability Statement

All data generated or used during this study are available from the corresponding author by reasonable request.

References

1 Singer M, Deutschman CS, Seymour CW *et al*. The Third International Consensus Definitions for Sepsis and Septic Shock (Sepsis-3). JAMA 2016; **315**:801–10.
2 Russell JA. Management of sepsis. N Engl J Med 2006; **355**:1699–713.
3 Fink MP, Warren HS. Strategies to improve drug development for sepsis. Nat Rev Drug Discov 2014; **13**:741–58.
4 Graetz TJ, Hotchkiss RS. Sepsis: preventing organ failure in sepsis – the search continues. Nat Rev Nephrol 2017; **13**:5–6.
5 Cecconi M, Evans L, Levy M, Rhodes A. Sepsis and septic shock. Lancet 2018; **392**:75–87.
6 Freudenberg MA, Galanos C. Induction of tolerance to lipopolysaccharide (Lps)-D-galactosamine lethality by pretreatment with Lps is mediated by macrophages. Infect Immun 1988; **56**:1352–7.
7 Benoit M, Desnues B, Mege J-L. Macrophage polarization in bacterial infections. J Immunol 2008; **181**:3733.
8 Gordon S, Martinez FO. Alternative activation of macrophages: mechanism and functions. Immunity 2010; **32**:593–604.
9 Chavez-Galan L, Olleros ML, Vesin D, Garcia I. Much more than M1 and M2 macrophages, there are also CD169(+) and TCR(+) macrophages. Front Immunol 2015; **6**:263.
10 Kumar V. Targeting macrophage immunometabolism: dawn in the darkness of sepsis. Int Immunopharmacol 2018; **58**:173–85.
11 Schneider CP, Schwacha MG, Chaudry IH. The role of interleukin-10 in the regulation of the systemic inflammatory response following trauma-hemorrhage. Biochim Biophys Acta 2004; **1689**:22–32.
12 Pena OM, Pistolic J, Raj D, Fjell CD, Hancock RE. Endotoxin tolerance represents a distinctive state of alternative polarization (M2) in human mononuclear cells. J Immunol 2011; **186**:7243–54.
13 Stehling O, Mascarenhas J, Vashisht AA *et al*. Human CIA2A-FAM96A and CIA2B-FAM96B integrate iron homeostasis and maturation of different subsets of cytosolic-nuclear iron-sulfur proteins. Cell Metab 2013; **18**:187–98.
14 Schwamb B, Pick R, Fernandez SBM *et al*. FAM96A is a novel pro-apoptotic tumor suppressor in gastrointestinal stromal tumors. Int J Cancer 2015; **137**:1318–29.
15 Yin A, Luo Y, Chen W *et al*. FAM96A protects mice from dextran sulfate sodium (DSS)-induced colitis by preventing microbial dysbiosis. Front Cell Infect Microbiol 2019; **9**:381.
16 Subashchandrabose S, Mobley HLT. Gentamicin protection assay to determine bacterial survival within macrophages. Bio-protocol 2014; **4**:e1235.
17 Sharma A, Puhar A. Gentamicin protection assay to determine the number of intracellular bacteria during infection of human TC7 intestinal epithelial cells by *Shigella flexneri*. Bio-Protocol 2019; **9**:e3292.
18 Buras JA, Holzmann B, Sitkovsky M. Animal models of sepsis: setting the stage. Nat Rev Drug Discov 2005; **4**:854–65.
19 Wichterman KA, Baue AE, Chaudry IH. Sepsis and septic shock – a review of laboratory models and a proposal. J Surg Res 1980; **29**:189–201.
20 Matute-Bello G, Downey G, Moore BB *et al*. An official American Thoracic Society workshop report: features and measurements of experimental acute lung injury in animals. Am J Respir Cell Mol Biol 2011; **44**:725–38.
21 Harrison C. Sepsis: calming the cytokine storm. Nat Rev Drug Discov 2010; **9**:360–1.
22 Delano MJ, Ward PA. The immune system's role in sepsis progression, resolution, and long-term outcome. Immunol Rev 2016; **274**:330–53.
23 Delano MJ, Ward PA. Sepsis-induced immune dysfunction: can immune therapies reduce mortality? J Clin Invest 2016; **126**:23–31.
24 Wolk K, Döcke WD, Von Baehr V, Volk HD, Sabat R. Impaired antigen presentation by human monocytes during endotoxin tolerance. Blood 2000; **96**:218–23.
25 Mills EL, Kelly B, Logan A *et al*. Succinate dehydrogenase supports metabolic repurposing of mitochondria to drive inflammatory macrophages. Cell 2016; **167**:457–470.e13.

26 Brieger K, Schiavone S, Miller FJ Jr, Krause KH. Reactive oxygen species: from health to disease. Swiss Med Wkly 2012; **142**:w13659.

27 Sena LA, Li S, Jairaman A *et al*. Mitochondria are required for antigen-specific T cell activation through reactive oxygen species signaling. Immunity 2013; **38**:225–36.

28 Petersen L, Nielsen GG, Andersen PK, Sorensen TI. Case–control study of genetic and environmental influences on premature death of adult adoptees. Genet Epidemiol 2002; **23**:123–32.

29 Sorensen TI, Nielsen GG, Andersen PK, Teasdale TW. Genetic and environmental influences on premature death in adult adoptees. N Engl J Med 1988; **318**:727–32.

30 Michie HR, Manogue KR, Spriggs DR *et al*. Detection of circulating tumor necrosis factor after endotoxin administration. N Engl J Med 1988; **318**:1481–6.

31 Mera S, Tatulescu D, Cismaru C *et al*. Multiplex cytokine profiling in patients with sepsis. APMIS 2011; **119**:155–63.

32 Panacek EA, Marshall JC, Albertson TE *et al*. Efficacy and safety of the monoclonal anti-tumor necrosis factor antibody F(ab(1)) (2) fragment afelimomab in patients with severe sepsis and elevated interleukin-6 levels. Crit Care Med 2004; **32**:2173–82.

33 Hsieh CS, Macatonia SE, Tripp CS, Wolf SF, Ogarra A, Murphy KM. Development of Th1 Cd4+ T cells through IL-12 produced by Listeria-induced macrophages. Science 1993; **260**:547–9.

34 Ramnath RD, Ng SW, Guglielmotti A, Bhatia M. Role of MCP-1 in endotoxemia and sepsis. Int Immunopharmacol 2008; **8**:810–18.

35 Copeland S, Warren HS, Lowry SF, Calvano SE, Remick D, Response IH. Acute inflammatory response to endotoxin in mice and humans. Clin Diagn Lab Immun 2005; **12**:60–7.

36 Hamidzadeh K, Christensen SM, Dalby E, Chandrasekaran P, Mosser DM. Macrophages and the recovery from acute and chronic inflammation. Annu Rev Physiol 2017; **79**:567–92.

37 Warburg O. On the origin of cancer cells. Science 1956; **123**:309–14.

38 Newsholme P, Curi R, Gordon S, Newsholme EA. Metabolism of glucose, glutamine, long-chain fatty acids and ketone bodies by murine macrophages. Biochem J 1986; **239**:121–5.

39 Jha Abhishek K, Huang Stanley C-C, Sergushichev A *et al*. Network integration of parallel metabolic and transcriptional data reveals metabolic modules that regulate macrophage polarization. Immunity 2015; **42**:419–30.

40 Vats D, Mukundan L, Odegaard JI *et al*. Oxidative metabolism and PGC-1β attenuate macrophage-mediated inflammation. Cell Metab 2006; **4**:13–24.

41 Huang SC-C, Everts B, Ivanova Y *et al*. Cell-intrinsic lysosomal lipolysis is essential for alternative activation of macrophages. Nat Immunol 2014; **15**:846–55.

42 Ganeshan K, Chawla A. Metabolic regulation of immune responses. Annu Rev Immunol 2014; **32**:609–34.

43 O'Neill LAJ, Hardie DG. Metabolism of inflammation limited by AMPK and pseudo-starvation. Nature 2013; **493**:346–55.

44 Tur J, Vico T, Lloberas J, Zorzano A, Celada A. Chapter One – macrophages and mitochondria: a critical interplay between metabolism, signaling, and the functional activity. In: Alt FW, ed. Advances in immunology. 133: Academic Press, 2017; 1–36.

45 Zhu L, Zhao Q, Yang T, Ding W, Zhao Y. Cellular metabolism and macrophage functional polarization. Int Rev Immunol 2015; **34**:82–100.

46 Pearce EL, Poffenberger MC, Chang CH, Jones RG. Fueling immunity: insights into metabolism and lymphocyte function. Science 2013; **342**:1242454.

47 Turrens JF. Mitochondrial formation of reactive oxygen species. J Physiol 2003; **552**:335–44.

48 Zhang Z, Deng W, Kang R *et al*. Plumbagin protects mice from lethal sepsis by modulating immunometabolism upstream of PKM2. Mol Med 2016; **22**:162–72.

Supporting Information

Additional supporting information may be found in the online version of this article at the publisher's web site:

Fig. S1. Location of PCR primers.

Fig. S2. Degree of knockout in *Fam96a*$^{-/-}$ mice validated using PCR and western blot. (a) Degree of knockout in *Fam96a*$^{-/-}$ mice validated using western blot analysis in the spleen. (b) Degree of knockout in *Fam96a*$^{-/-}$ mice validated using PCR. For KO-1 primers, the extension time of the indicated PCR programme is insufficient for the synthesis of a new DNA chain in wild-type (WT) mice.

Fig. S3. The differentiation efficiency of bone-marrow-derived macrophage (BMDMs).